PCCP

Accepted Manuscript

This is an *Accepted Manuscript*, which has been through the Royal Society of Chemistry peer review process and has been accepted for publication.

Accepted Manuscripts are published online shortly after acceptance, before technical editing, formatting and proof reading. Using this free service, authors can make their results available to the community, in citable form, before we publish the edited article. We will replace this *Accepted Manuscript* with the edited and formatted *Advance Article* as soon as it is available.

You can find more information about *Accepted Manuscripts* in the Information for Authors.

Please note that technical editing may introduce minor changes to the text and/or graphics, which may alter content. The journal's standard Terms & Conditions and the Ethical guidelines still apply. In no event shall the Royal Society of Chemistry be held responsible for any errors or omissions in this *Accepted Manuscript* or any consequences arising from the use of any information it contains.

ROYAL SOCIETY OF CHEMISTRY

www.rsc.org/pccp

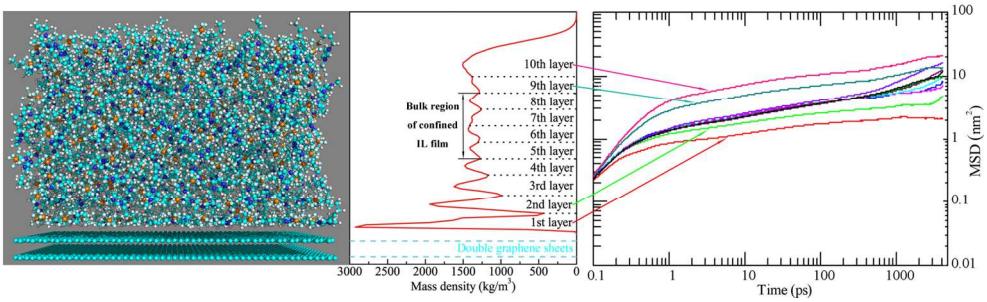

Physical Chemistry Chemical Physics Accepted Manuscript

ARTICLE TYPE
www. rsc.org/xxxxxx | XXXXXXXX

Heterogeneous Dynamics of Ionic Liquid in Confined Films with Varied Film Thickness

Yong-Lei Wang[*a], **Zhong-Yuan Lu**[b] **and Aatto Laaksonen**[*a,c]

Received Xth XXXXXXXXXX 20XX, Accepted Xth XXXXXXXXX 20XX
First published on the web Xth XXXXXXXXXX 200X
DOI: 10.1039/b000000x

Dynamical behavior and characteristics of 1-butyl-3-methylimidazolium hexafluorophosphate ([BMIM][PF_6]) ionic liquid (IL) in confined films with varied film thickness have been investigated using atomistic Molecular Dynamics simulations. Simulation results indicate that the dynamics of confined ionic groups in interfacial regions is highly heterogeneous and depends strongly on their relative layered positions in the confined IL film. The dynamics and relaxation times of the ionic groups in the bulk region of confined IL film are very similar to that in corresponding pure bulk simulation. In contrast, the diffusion of corresponding ionic groups slows down and can be characterized as slaved diffusion while corresponding relaxation times increase remarkably as these ionic groups come closer to the neutral graphene surface. While at the IL-vacuum interface, the diffusion and relaxation of terminal carbon atoms of butyl chains of [BMIM] cations are much faster than in other layers of the confined IL film and in the bulk region of simulation system without confinement, due to their librated motion in this interfacial region. The dynamical heterogeneity of the confined ionic groups is intrinsically related to microscopic ionic structures and orientational preference of [BMIM][PF_6] ion pairs in interfacial regions.

1 Introduction

Room-temperature ionic liquids (ILs) are special categories of molten salts composed exclusively of organic cations and, most commonly, inorganic anions, having their melting points at or close to room temperature[1]. Due to their excellent thermal stability, nonvolatility, and wide electrochemical window, several groups[2–6] have recently applied ILs as green versatile solvents for chemical synthesis and catalysis[7,8], and as alternative electrolytes for electrochemistry[6,9] and photovoltaics[10,11], such as in electrochemical double-layer capacitors (EDLCs) and dye-sensitized solar cells (DSSCs)[6,12–16] for the conversion of solar energy. In these particular applications, the macroscopic performance of IL-based EDLCs and DSSCs is fundamentally determined by the microscopic structural and dynamical properties of ion pairs in the interfacial region[2,5,17,18], where the physicochemical properties of confined ionic species are found to be totally different from those in bulk region. Hence, a fundamental understanding of the interfacial properties of ILs is crucial for rational design of EDLCs and DSSCs, and improving their functional performance in multiphase applications. Molecular simulations, in close interplay with experiments, are well positioned to provide fundamental understanding and advance IL-based technologies beyond their current state of the art.

Recent computer simulation studies have focused on the absorption of ILs on various solid surfaces, such as rutile[19,20], graphene[21–24], quartz[25,26] and sapphire[27,28], and inside regulated nanopores with slitlike[20,29–32] and cylindrical geometries[33–35], as well as inside nanoporous materials[36,37]. Hung and coworkers studied the structural and dynamical properties of confined ILs inside multiwalled carbon nanotubes[35], slitlike graphitics[30,32,38], and rutile nanopores[20]. They found that the ionic structures and dynamics of confined ionic groups inside a nanoporous electrode were very complex and described by heterogeneous characteristics. Both local ionic structures and diffusion of confined ion pairs in the vicinity of solid surface can severely affect macroscopic capacitance of electrochemical devices.

In a recent study, we systematically performed atomistic Molecular Dynamics simulations to study the microscopic structures and orientational preference of 1-butyl-3-methylimidazolium hexafluorophosphate ([BMIM][PF_6]) in IL-graphene and IL-vacuum interfacial regions[24]. Several stable dense layers with pronounced density distributions were formed at IL-graphene interface. The imidazolium rings of [BMIM] cations lied preferentially flat on graphene surface, with corresponding methyl and butyl chains elongated along the neutral surface. While at the IL-vacuum interface, interfacial monolayer with distinct ionic structures was formed, in

[a] *Department of Materials and Environmental Chemistry, Arrhenius Laboratory, Stockholm University, Stockholm S-106 91, Sweden; E-mail: yonglei.wang@mmk.su.se; aatto.laaksonen@mmk.su.se.*
[b] *Institute of Theoretical Chemistry, State Key Laboratory of Theoretical and Computational Chemistry, Jilin University, Changchun 130023, China.*
[c] *Stellenbosch Institute of Advanced Studies (STIAS), Wallenberg Research Center, Stellenbosch University, Stellenbosch 7600, South Africa.*

Physical Chemistry Chemical Physics Accepted Manuscript

which [BMIM] cations and [PF_6] anions were packed closely together to form polar domains beneath the exposed IL-vacuum interface. The orientation of [BMIM] cations in such a monolayer changed gradually from dominant flat distribution to that characterized by several favorable orientation in different proportions with the increase of film thickness. The exposed outmost layer was populated with alkyl groups and imparted with distinct hydrophobic characteristics. The local ionic structures in IL-graphene and IL-vacuum interfacial regions were significantly different to that in the bulk region of confined IL film, attributing to the striking arrangement of polar and nonpolar domains in interfacial regions, and leading to the confined IL film characterized by interfacial structural heterogeneity, which is intrinsically related to complex dynamical behavior of [BMIM][PF_6] in interfacial regions.

In the present study, we explore the dynamical properties of [BMIM][PF_6] IL in confined films characterized by varied film thickness. The atomistic simulation results of velocity autocorrelation functions, mean square displacements, and time-dependent self-part of van Hove correlation functions of three typical ionic groups are reported in detail. Meantime, these dynamical properties are compared to those calculated from simulation system without confinement used as a reference. These dynamical properties have been proven useful to detect and characterize dynamical heterogeneity of neat IL simulation systems[39,40] and supercooled Lennard-Jones liquids confined in a slit pore[41].

2 Simulation method

The detailed procedures of constructing double-layer graphene sheets and the initial configuration of [BMIM][PF_6] IL on graphene surface were described in our previous work[24]. Taking the confined film consisting of 500 [BMIM][PF_6] ion pairs for example, we built such film by repeating the equilibrated IL monolayer consisting of 50 [BMIM][PF_6] ion pairs 10 times along Z-axis.

Atomistic Molecular Dynamics simulations were performed using the DL_POLY package[42]. The equations of motion were integrated using the Verlet leapfrog algorithm with a time step of 1.0 fs. The Ewald summation method with an accuracy of 10^{-5} and a real space cutoff of 1.2 nm was adopted to calculate the electrostatic interactions between atom-centered point charges. The cutoff radius of van der Waals interactions was set to 1.2 nm for computational efficiency. All systems were simulated in NVT ensemble at 300 K maintained by Nosé-Hoover thermostat for 10 ns, and statistical data from the last 6 ns were collected for further analysis.

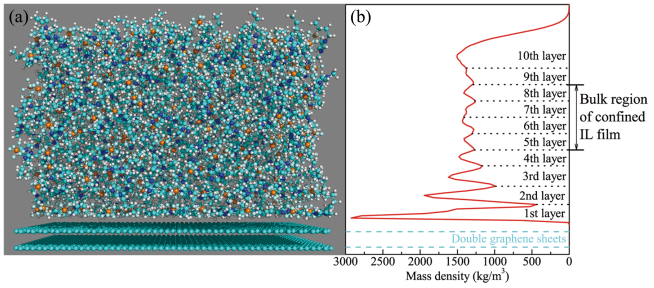

Fig. 1 (a) Representative snapshot of the confined IL film consisting of 500 [BMIM][PF_6] ion pairs on neutral graphene surface. (b) This film can be divided into 10 layers based on the mass density profile.

3 Results and Discussion

For the confined film consisting of 500 [BMIM][PF_6] ion pairs, the total mass density distribution is shown in Fig. 1. On the basis of this density profile, we can split this IL film into 10 layers according to the relative distance between [BMIM][PF_6] ion pairs and graphene surface. The $1st$ layer is the bottom layer close to graphene surface, and the $10th$ layer corresponds to the outmost layer in IL-vacuum interface. The $5th$, $6th$, $7th$, and $8th$ layers, in which the mass densities are similar to the bulk density of simulation system without confinement, are considered as the bulk region of this IL film. In present atomistic simulations, we have monitored the coordinates of center-of-mass (COM) of imidazolium rings and geometrical centers of [PF_6] anions as a function of simulation time. We have not observed noticeable exchange of these ionic groups between adjacent layers in IL-graphene and IL-vacuum interfacial regions, which facilitates the sampling and calculation of dynamic properties of corresponding ionic groups in interfacial regions. The statistical analysis of following dynamical properties is performed for ionic groups in corresponding layers in the whole simulation scheme.

3.1 Velocity autocorrelation functions

The dynamical behavior and microscopic motion of different groups are first studied by calculating the normalized velocity autocorrelation functions (VACFs), $\hat{C}_v(t)$, of the center-of-mass (COM) of three ionic groups from trajectories. The VACF is defined as

$$\hat{C}_v(t) = \frac{\langle \mathbf{v}^c(0) \cdot \mathbf{v}^c(t) \rangle}{\langle \mathbf{v}^c(0) \cdot \mathbf{v}^c(0) \rangle}, \quad (1)$$

where $\mathbf{v}^c(t)$ are the COM velocity vectors of imidazolium rings and terminal carbon atoms of butyl chains of [BMIM] cations, as well as [PF_6] anions. The angular brackets $\langle\rangle$ represent an ensemble average over ionic groups in corresponding layers in simulation system.

This journal is © The Royal Society of Chemistry [year]

Physical Chemistry Chemical Physics Accepted Manuscript

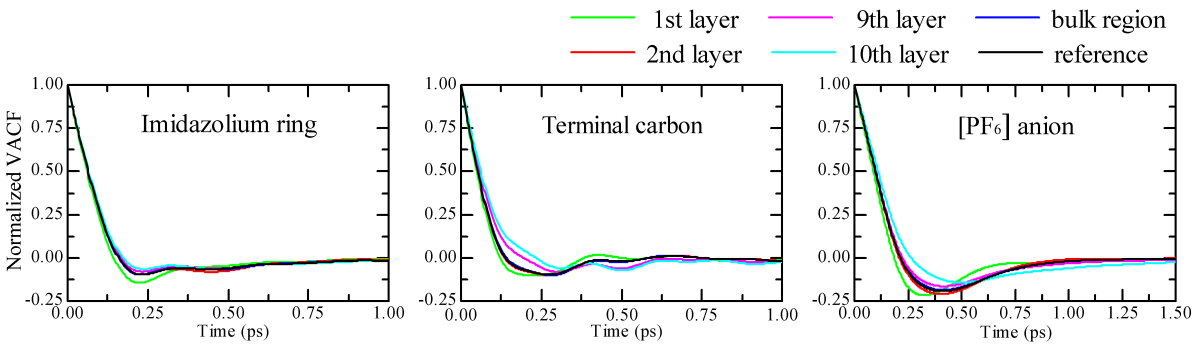

Fig. 2 Normalized VACFs of imidazolium rings and terminal carbon atoms of butyl chains of [BMIM] cations, and $[PF_6]$ anions in different layers of confined IL film consisting of 500 [BMIM]$[PF_6]$ ion pairs, as well as in simulation system without confinement.

For the confined film consisting of 500 [BMIM]$[PF_6]$ ion pairs, the normalized VACFs of three ionic groups in the 1*st* and 2*nd* layers at IL-graphene interface, and in the 9*th* and 10*th* layers at IL-vacuum interface, are calculated from trajectories and shown in Fig. 2. These VACFs are compared to corresponding counterparts calculated from the bulk region of the same film (as depicted in Fig. 1), as well as to those obtained from simulation system without confinement.

For three ionic groups in different layers of this film, as well as in bulk region of simulation system without confinement, the time scale of corresponding normalized VACFs shows a similar general feature. The first zero values in these VACFs are approximately at $0.12 - 0.30$ ps, which indicates a measurement of the mean collision time of corresponding ionic groups. All these VACFs have negative regions after the mean collision time, corresponding to their rattling motion within a cage formed by surrounding counterions. The minima of these VACFs locate at around 0.2 ps and 0.3 ps for imidazolium rings and terminal carbon atoms of butyl chains of [BMIM] cations, and approximately 0.4 ps for $[PF_6]$ anions, respectively. Then these VACFs oscillate around zero, which is considered as a measurement of the velocity randomization time of corresponding ionic groups. The mean collision time and the velocity randomization time of three ionic groups follow the order of $[PF_6]$ anion $>$ imidazolium ring $>$ terminal carbon atom. The terminal carbon atom of butyl chain is much lighter than imidazolium ring and $[PF_6]$ anion, and hence its VACF exhibits distinct and clear oscillation in intermediate time between the mean collision time and the velocity randomization time. Such observation implies the effect of relative mass of ionic group on VACF oscillation, as has been discussed by Rey-Castro and coworkers[43] in detail.

The short-time translational modes of the three ionic groups in different layers show distinct characteristics from one to another. In the IL-graphene interface, the effect of neutral graphene surface on VACFs is short-ranged and only important in the 1*st* layer. In such layer, the VACFs of the three ionic groups decay much more quickly than the corresponding ionic groups in other layers, and follow the order of inverse of corresponding relative mass as terminal carbon atom $>$ imidazolium ring $>$ $[PF_6]$ anion. While in the outmost layer (the 10*th* layer), the three ionic groups show slow VACF decay (which is also observed in the confined IL film consisting of 300 [BMIM]$[PF_6]$ ion pairs; data not shown), owing to the distinct ionic structures formed in IL-vacuum interfacial region. For ionic groups in the 2*nd* and 9*th* layers, as well as in the bulk region of this film, their VACFs show intermediate decay and locate between VACFs of ionic groups in the 1*st* layer at IL-graphene interface and the 10*th* layer at IL-vacuum interface. These VACFs are consistent with those deduced from simulation system without confinement, attributing to the short-ranged confinement effect induced by neutral graphene surface. When the neutral graphene surface is replaced by positively or negatively charged surface, such as mica[44], quartz[25], and sapphire[27] surfaces, the influence of charged solid surface on VACFs of confined [BMIM]$[PF_6]$ ion pairs extends to the 2*nd* layer, or even the 3*rd* layer in the vicinity of solid surface.

For confined IL films characterized with varied film thickness, the VACFs of three ionic groups in the 1*st* and the outmost layers are calculated and presented in Fig. 3, as well as corresponding VACFs deduced from simulation system without confinement. All VACFs of the three ionic groups in the 1*st* layer of confined films consisting of 100, 150, 200, 300, and 500 [BMIM]$[PF_6]$ ion pairs show similar features, owing to the short-ranged confinement effect induced by the neutral graphene surface. While in the outmost layer of these simulated systems, distinct VACFs can be observed, but the difference between these VACFs becomes negligible with the increase of film thickness. For the confined film consisting of 50 [BMIM]$[PF_6]$ ion pairs, there is only one IL layer formed on graphene surface. In this case the monolayer serves both as an IL-graphene and an IL-vacuum interface. The VACFs of the three ionic groups in such monolayer exhibit distinct tenden-

Physical Chemistry Chemical Physics Accepted Manuscript

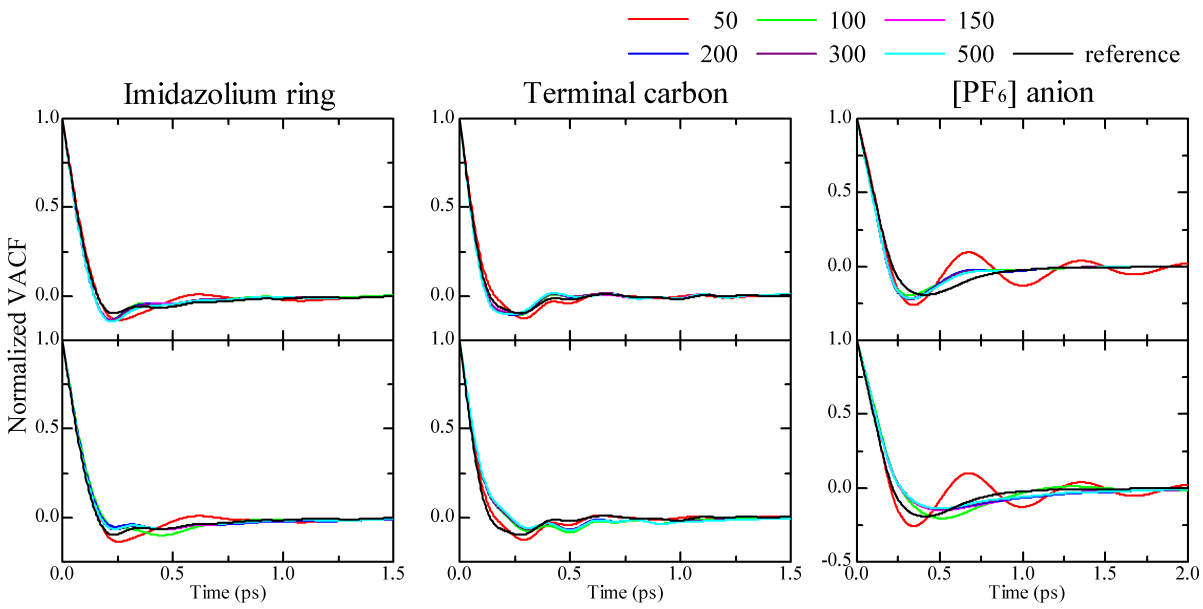

Fig. 3 Normalized VACFs of imidazolium rings and terminal carbon atoms of butyl chains of [BMIM] cations, and [PF_6] anions in the 1*st* layers (top row) and the outmost layers (bottom row) of confined IL films with varied film thickness, as well as corresponding VACFs deduced from simulation system without confinement.

cies compared to that in the 1*st* layer on graphene surface and counterpart VACFs of ionic groups in the outmost layer at IL-vacuum interface. Such striking observation can be attributed to the two-dimensional mesophase formed by [BMIM] cations and [PF_6] anions with short-ranged and regulated ionic structures in the vicinity of IL-graphene interface, as reported in previous work[24].

3.2 Mean square displacements

For a liquid or solution at thermodynamic equilibrium conditions, the thermal agitation causes translational motion of liquid molecules, called self-diffusion[39,40]. From the molecular point of view, self-diffusion of molecules gives detailed microscopic description of single-particle motion. Molecular mass transport properties can be calculated from the integrals of flux time-correlation functions via the Green-Kubo formulas[39,40]. Alternatively, these properties can also be obtained from generalized mean square displacements (MSDs). These two methods are rigorously equivalent but are subject to different numerical errors in finite time simulations of finite size systems. Herein, we investigate the diffusion of confined ionic groups by calculating corresponding MSD, which is defined as

$$MSD = \frac{1}{N}\langle \sum_{i=1}^{N} |\mathbf{r}_i^c(t) - \mathbf{r}_i^c(0)|^2 \rangle , \qquad (2)$$

where $\mathbf{r}_i^c(t)$ are the COM coordinates of the ith molecule at time t. The MSDs of three ionic groups are calculated from trajectories with a time interval of 100 fs in present atomistic simulations.

For the confined film consisting of 500 [BMIM][PF_6] ion pairs, the calculated MSDs of imidazolium rings and terminal carbon atoms of butyl chains of [BMIM] cations, as well as [PF_6] anions, in different layers are presented in Fig. 4. The diffusion of the three ionic groups is strongly related to their relative positions in this film, and their dynamics is strongly heterogeneous. All MSDs exhibit three distinct dynamical regimes: the ballistic, sub-diffusive, and diffusive regimes[30,41,45]. The ballistic regime covers in a few ps, in which the ionic groups have not interacted with their surrounding neighbors, and thus their diffusion is described as MSD $\propto \Delta t^2$, which is faster than that in the other two regimes.

After the ballistic regime, a plateau which extends to more than 1000 ps is observed in each MSD plot, implying that each simulation system is in the sub-diffusive regime, in which the diffusion of the ionic groups slows down since they are trapped within a cage formed by surrounding counterions. In this regime, the dynamics of ionic groups is described by MSD $\propto \Delta t^{\alpha}$ with $0 < \alpha < 1$. For the ionic groups in the 1*st* layer of confined IL film, the time window of the MSD plateau is much larger than that in other layers. While the time windows of plateaus of ionic groups in the 2*nd*, 3*rd* and 4*th* layers become slightly smaller depending on their relative distance

This journal is © The Royal Society of Chemistry [year]

Physical Chemistry Chemical Physics Accepted Manuscript

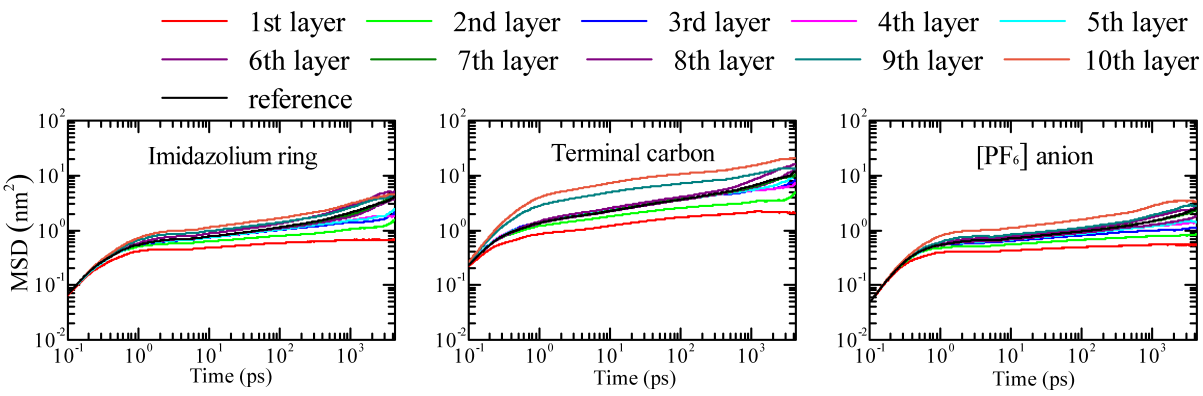

Fig. 4 The MSDs of imidazolium rings and terminal carbon atoms of butyl chains of [BMIM] cations, and $[PF_6]$ anions in different layers of confined IL film consisting of 500 [BMIM][PF_6] ion pairs, as well as in simulation system without confinement.

from graphene surface. In the bulk region of this film, the diffusion of all three ionic groups is generally consistent with that deduced from simulation system without confinement. A striking feature is observed for the ionic groups in top two layers, that is the $9th$ and $10th$ layers in this film as shown in Fig. 1, the dynamics of terminal carbon atoms shows distinct characteristics compared to that of imidazilium rings and $[PF_6]$ anions, attributing to the heterogeneous ionic structures in IL-vacuum interfacial region. As discussed in our previous work[24], an interfacial layer with distinct density distribution and ionic structures is formed at IL-vacuum interface. The exposed IL-vacuum surface is populated with alkyl groups (mainly butyl chains), leading to the librated motion of terminal carbon atoms of butyl chains in interfacial region. Beneath such exposed outmost layer, imidazolium rings and $[PF_6]$ anions are closely packed together to form polar domains due to strong electrostatic interactions, which resembles microscopic ionic structures in the bulk region of this confined film. Such structural similarity leads to analogous diffusion as that in the bulk region of confined IL film, and that in simulation system without confinement.

Eventually, ionic groups escape the trapped cage, and corresponding simulation systems reach the diffusive regime, in which the diffusion is characterized by MSD $\propto \Delta t$. Comparing to the ionic groups in other layers of this confined film, the ones in the $1st$ layer exhibit the slowest dynamics, and hence spend the longest time in the sub-diffusive regime. As shown in Fig. 4, we cannot observe the transition from the sub-diffusive to diffusive regimes even in very long atomistic simulations. By further inspection, we find that the slopes of corresponding plateaus are small (but larger than zero), similar to the simulation results for supercooled Lennard-Jones liquids confined in slit pore with rough walls[41], which is indicative of analogically slaved diffusion. The ionic groups in the bulk region of confined IL film and in simulation system without confinement exhibit similar dynamical feature and reach the diffusive regime much faster than that in IL-graphene interface. These simulation results present consistent tendencies with previous atomistic simulation results for confined ion pairs in cylindrical pores[20,35] and nanoslits[30,32,38]. In contrast, the ionic groups in top two layers of IL-vacuum interface exhibit distinct diffusion compared to that in IL-graphene interface, as well as to that in the bulk region of this confined film and in simulation system without confinement, attributing to the heterogeneous ionic structures in IL-vacuum interfacial region.

The self-diffusion coefficients of [BMIM] cation and $[PF_6]$ anion in the bulk region of this confined film, obtained from MSDs in typical diffusive regime using the Einstein relation, are approximately $(1.41 \pm 0.03) \times 10^{-11}$ m^2/s and $(1.13 \pm 0.02) \times 10^{-11}$ m^2/s, respectively. These simulation results are consistent with that calculated using formally equivalent Green-Kubo formulas, in which it is assumed that the integrals of VACFs decay exponentially at long time, as well as that reported in previous atomistic simulations[30,46].

The confinement effect induced by neutral graphene surface on the same IL film is not only embodied in overall diffusion of ionic groups in different layers, but also depicted in different MSD components of the ionic groups in the same layer. The XY parallel and Z perpendicular MSD components of three ionic groups in the $1st$ and $2nd$ layers, the bulk region, and the $10th$ layer of this confined film, are respectively shown in Fig. 5. Meantime, the MSD components of the corresponding ionic groups in XY plane and Z direction are also obtained for the simulated system without confinement for a better comparison.

For ionic groups in the $1st$ and $2nd$ layers, their diffusion in Z direction is much slower as compared to XY component due to the confinement effect induced by graphene surface. Such confinement effect, not only triggered by solid planar surface,

Physical Chemistry Chemical Physics Accepted Manuscript

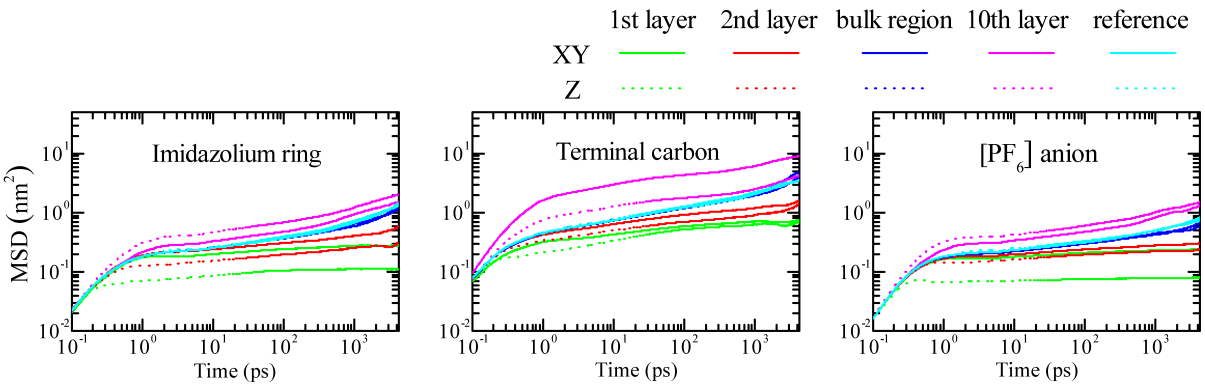

Fig. 5 The XY parallel and Z perpendicular MSD components of imidazolium rings and terminal carbon atoms of butyl chains of [BMIM] cations, and [PF_6] anions in the 1*st* and 2*nd* layers, the bulk region, and the 10*th* layer of confined IL film consisting of 500 [BMIM][PF_6] ion pairs, as well as in simulation system without confinement.

such as quartz[47], silica[26,48], graphene[30,32,38,49–51], and metal surfaces[52], but also induced by single- and multi-walled carbon nanotubes[34,35,45], and mesoporous CMK-3 carbon materials[37], directly contributes to the heterogeneous dynamics in parallel plane and perpendicular direction. But such confinement effect becomes weak with the increase of relative distance between ionic groups and graphene surface, resulting in comparable MSD components in XY parallel plane and Z perpendicular direction, as clearly shown in Fig. 5. In the outmost layer, the distinct dynamics of the ionic groups in XY parallel plane and Z perpendicular direction attributes to the heterogeneous ionic structures in IL-vacuum interfacial region.

In all layers outlined in Fig. 5, the diffusion of terminal carbon atoms of butyl chains of [BMIM] cations is much faster than that of imidazolium rings and [PF_6] anions. This attributes to the local ionic structures characterized by connected polar network formed by imidazolium rings and [PF_6] anions, and isolated apolar domains formed by methyl groups of [BMIM] cations. In isolated apolar domains, terminal carbon atoms are surrounded by other apolar methyl groups in butyl chains, which facilitates their overall diffusion. While in connected polar network, imidazolium rings and [PF_6] anions are strongly coupled together through electrostatic interactions, which contributes to their slow diffusion. Furthermore, it is also observed that imidazolium rings diffuse faster than [PF_6] anions, independent of their relative distance from graphene surface. Such phenomena had been reported in bulk region of imidazolium-based ILs[39,53], and rationalized by a preferential displacement of imidazolium ring along the carbon-hydrogen direction between two nitrogen atoms.

For confined IL films characterized by varied film thickness, the diffusion of the three ionic groups exhibits striking behavior as even these ionic groups locate in the same layer but in different simulation systems. In Fig. 6, we illustrate the MSDs of three ionic groups in the 1*st* and the outmost layers, respectively, as well as that deduced from simulation system without confinement.

For [BMIM] cations and [PF_6] anions in the 1*st* layer of confined films consisting of 100, 150, 200, 300 and 500 ion pairs, their overall dynamics exhibits similar tendency. In the sub-diffusion regime, the time window of corresponding plateau is larger than that in bulk region of simulation system without confinement. Even the slope of each plateau varies from one to another, all ionic groups in the 1*st* layer are in the sub-diffusion regime in whole simulation scheme. While in the outmost layer of these confined films, the MSDs of ionic groups exhibit remarkable and distinguishable feature compared to the reference MSDs deduced from simulation system without confinement. The striking dynamical properties of ionic groups in IL-vacuum interface are considered as a competition between their interactions with neutral graphene surface and their cohesion behavior (surface tension).

For the ionic groups in the confined film consisting of 50 [BMIM][PF_6] ion pairs, the overall diffusion of three ionic groups exhibits remarkable difference with respect to corresponding counterparts in the same layer but different simulation systems. In this special IL monolayer, imidazolium rings and butyl chains of [BMIM] cations prefer to take parallel orientation, which is much more energetically favorable than other conformations. Meantime, the [PF_6] anions locate around imidazolium rings due to strong electrostatic interactions. On one side, the preferential distribution of [BMIM] cations in this monolayer, which is a compromise between their interactions with graphene surface and their orientational preference in IL-vacuum interface, restricts the diffusion of [BMIM] cations along graphene surface. On the other side, the special local ionic structures further limit the diffusion of imidazolium rings and [PF_6] anions along graphene surface, as depicted

This journal is © The Royal Society of Chemistry [year]

Physical Chemistry Chemical Physics Accepted Manuscript

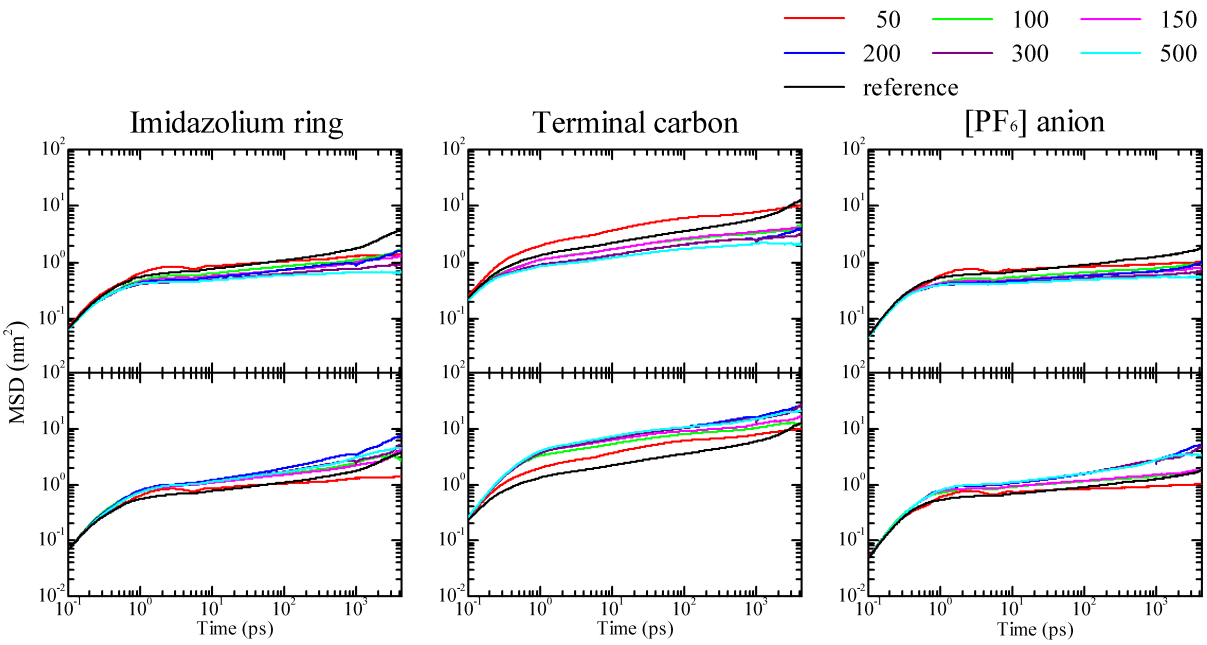

Fig. 6 The MSDs of imidazolium rings and terminal carbon atoms of butyl chains of [BMIM] cations, and [PF_6] anions in the 1*st* layers (top row) and the outmost layers (bottom row) of confined IL films with varied film thickness, as well as corresponding MSDs deduced from simulation system without confinement.

in top row of Fig. 6. The intrinsic microscopic ionic structures and preferential distribution of [BMIM][PF_6] ion pairs in this monolayer lead to compromised dynamics compared to that of ionic groups in the same outmost layer but different simulation systems, as depicted in bottom row of Fig. 6.

3.3 Self-part of van Hove correlation function

The simulation results from previous subsections show that the dynamics of [BMIM] cations and [PF_6] anions is heterogeneous and depends on their relative positions in confined IL films. Since the MSDs give typical average distance that a tagged ionic group moves within a time t, it is of interest to investigate the distribution of its displacement, which can be quantified by computing the time-dependent self-part of van Hove correlation function $G_s(r,t)$ as [30,40]

$$G_s(r,t) = \frac{1}{N}\sum_{i=1}^{N}\langle \delta[\mathbf{r}+\mathbf{r}_i(t)-\mathbf{r}_i(0)]\rangle . \qquad (3)$$

The function $4\pi r^2 G_s(r,t)$ is the probability that within the time t a particle has moved a distance r away from the place it was at $t = 0$. In following, the self-part of van Hove correlation function $G_s(r,t)$ and function $4\pi r^2 G_s(r,t)$ of the ionic groups in different layers of the confined film consisting of 500 [BMIM][PF_6] ion pairs, as well as in the reference system from the simulation without confinement, are calculated within three characteristic regimes.

At short time $t = 0.1$ ps, all simulation systems are in the ballistic regime, as depicted in Fig. 4, therefore the $G_s(r,t)$ of the three ionic groups, irrespective of their relative positions in confined IL film, shows a similar tendency and decays rapidly to zero at a very short distance, as shown in Fig. 7. The decay of $G_s(r,t)$ follows the order of [PF_6] anion > imidazolium ring > terminal carbon atom, consistent with the mean collision time and the velocity randomization time of the corresponding ionic groups in VACF plots. In bottom row of Fig. 7, the $4\pi r^2 G_s(r,t)$ of the ionic groups in the bulk region of this confined film exhibits Gaussian-like characteristics at short time $t = 0.1$ ps.

In Fig. 8, we present the $4\pi r^2 G_s(r,t)$ of three ionic groups at intermediate time $t = 10$ ps and long time $t = 1000$ ps, when the simulation system without confinement is in the sub-diffusive and diffusive regimes, respectively. The general feature is that the peak positions of $4\pi r^2 G_s(r,t)$ shift gradually to large distance compared to that in short time as time increases, indicative of the transition of ionic liquid diffusion from the ballistic to sub-diffusive and diffusive regimes.

For simulations at intermediate time $t = 10$ ps, the peak positions of $4\pi r^2 G_s(r,t)$ of the ionic groups in the 1*st* layer are at around 0.081 nm for imidazolium rings and [PF_6] anions, and 0.118 nm for terminal carbon atoms of butyl chains, respectively. All these peak positions are at short distances

Physical Chemistry Chemical Physics Accepted Manuscript

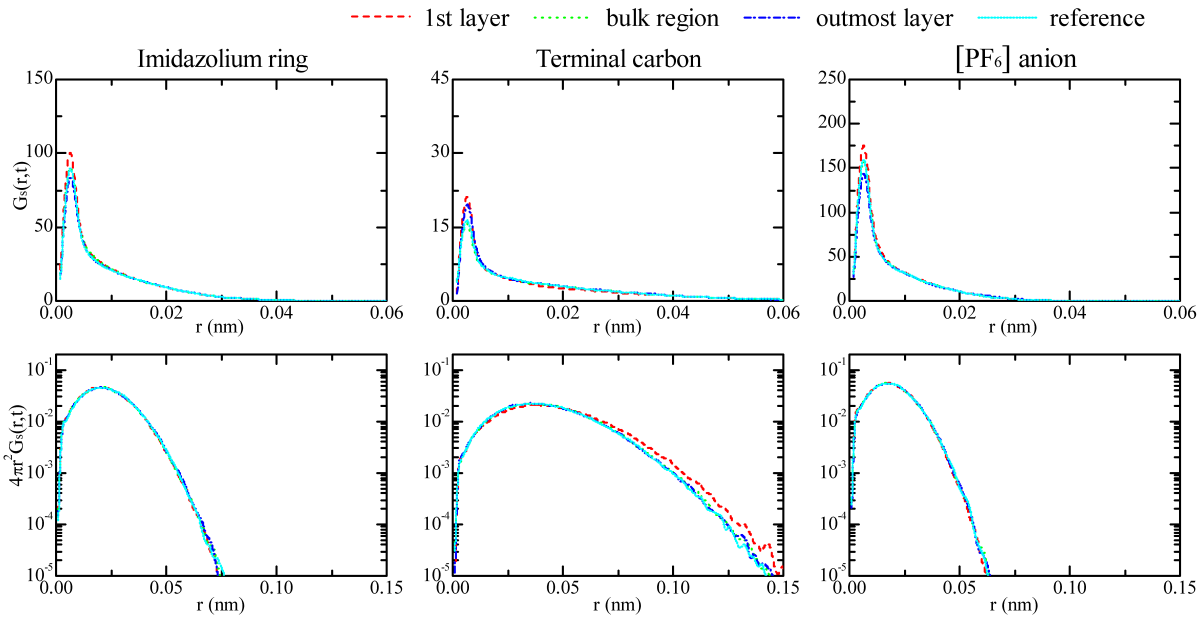

Fig. 7 The self-part of the van Hove correlation function $G_s(r,t)$ (top row) and function $4\pi r^2 G_s(r,t)$ (bottom row) of imidazolium rings and terminal carbon atoms of butyl chains of [BMIM] cations, and [PF_6] anions at short time $t = 0.1$ ps in the 1*st* layer, the bulk region, and the outmost layer of confined IL film consisting of 500 [BMIM][PF_6] ion pairs, as well as in simulation system without confinement.

compared to those of the corresponding ionic groups in other layers, highlighting again the fact that the ionic groups close to the graphene surface exhibit distinct dynamics which is much slower than that in the bulk region of this confined film and simulation system without confinement. The maxima of $4\pi r^2 G_s(r,t)$, coupled with the MSD results in Fig. 4, indicate that at intermediate time $t = 10$ ps the ionic groups in the 1*st* layer have not yet left the initial cage formed by their surrounding counterions at initial time $t = 0$ ps. With the increase of relative distance between the ionic groups and the graphene surface, the peak positions of $4\pi r^2 G_s(r,t)$ gradually shift towards large distances. The ionic groups in the bulk region of this confined film and simulation without confinement show similar feature in $4\pi r^2 G_s(r,t)$ curves. Both of them exhibit Gaussian-like behavior, but significant deviations are observed for the ionic groups in the IL-graphene and IL-vacuum interfacial regions. For the terminal carbon atoms of butyl chains of [BMIM] cations in the outmost layer, the corresponding $4\pi r^2 G_s(r,t)$ plots have non-negligible values even for r larger than 1.0 nm, indicating that these terminal carbon atoms have left the cage in which they were at time $t = 0$ ps. While for imidazolium rings and [PF_6] anions in IL-vacuum interfacial region, the corresponding $4\pi r^2 G_s(r,t)$ curves are still localized at a distance around 0.5 nm, *i.e.*, these two ionic groups have not yet left their initial cage at intermediate time $t = 10$ ps.

While at long time $t = 1000$ ps, all $4\pi r^2 G_s(r,t)$ plots of the ionic groups in different layers show heterogeneous dynamics in the confined film consisting of 500 [BMIM][PF_6] ion pairs. The multiple peaks in $4\pi r^2 G_s(r,t)$ curves indicate that a weak activated hopping process occurs in throughout the simulation, *i.e.*, one ionic group leaves one cage and enters another, which results in appearance of secondary peaks in $4\pi r^2 G_s(r,t)$ curves at large distance and long time, as reported in supercooled Lennard-Jones liquids confined in slit pore with rough walls[41].

For [BMIM] cations and [PF_6] anions in the 1*st* and the outmost layers of confined films consisting of 100, 150, 200, 300, and 500 [BMIM][PF_6] ion pairs, their dynamics shows similar features due to the short-range confinement effect induced by neutral graphene surface, as discussed in previous subsections. For the ionic groups in the IL layer of confined film consisting of 50 [BMIM][PF_6] ion pairs, their dynamics shows a similar tendency as that in VACFs and MSDs, mainly attributing to the local ionic structures in IL-graphene and IL-vacuum interfacial regions.

4 Summary and conclusion

Atomistic Molecular Dynamics simulations have been performed to study the dynamical behavior of [BMIM][PF_6] ion pairs in confined films with varied film thickness on neutral graphene surface. Detailed analysis using velocity auto-

This journal is © The Royal Society of Chemistry [year]

Physical Chemistry Chemical Physics Accepted Manuscript

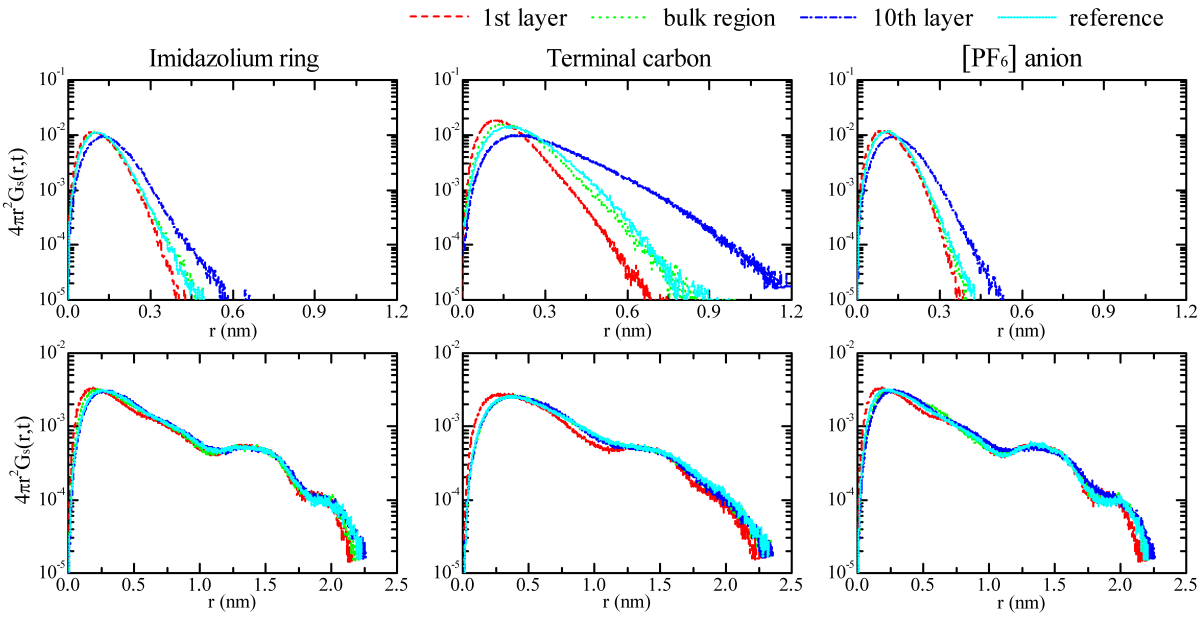

Fig. 8 Function $4\pi r^2 G_s(r,t)$ for imidazolium rings and terminal carbon atoms of butyl chains of [BMIM] cations, and [PF_6] anions at intermediate time $t = 10$ ps (top row) and long time $t = 1000$ ps (bottom row) in the 1*st* layer, the bulk region, and the outmost layer of confined IL film consisting of 500 [BMIM][PF_6] ion pairs, as well as in simulation system without confinement.

correlation functions, mean square displacements and time-dependent self-part of van Hove correlation functions, of confined [BMIM][PF_6] ion pairs in different layers indicate that the diffusion of these ionic groups is highly heterogeneous, and strongly depends on their relative positions in confined IL film. At the IL-graphene interface, the dynamical heterogeneity of ionic groups is not only embodied in their overall diffusion, but also represented in the diffusive components in parallel (XY) plane along graphene surface and in perpendicular (Z) direction. The overall diffusion of [BMIM][PF_6] ionic groups is characterized with slaved diffusion, and it takes much longer time for these confined ionic groups to leave the cage formed by surrounding counterions before finally reaching the diffusive regime. While in IL-vacuum interface, the diffusion and relaxation of terminal carbon atoms of butyl chains of [BMIM] cations are much faster than that in other layers due to their librated motion in IL-vacuum interfacial region.

The striking dynamical heterogeneity is intrinsically related to the orientational preference and microscopic ionic structures of [BMIM][PF_6] ion pairs in IL-graphene and IL-vacuum interfacial regions. The confinement effect induced by neutral graphene surface and the two-dimensional mesophase formed by [BMIM] cations and [PF_6] anions contribute to the slaved diffusion of confined ion pairs in IL-graphene interfacial region. But such confinement effect is short-ranged, and its influence on dynamical property is only limited in the bottom layer of confined IL film, and becomes negligible with the increase of film thickness. For thick enough confined IL film, such as the one consisting of 500 [BMIM][PF_6] ion pairs, the exposed outmost layer is populated with alkyl groups, mainly terminal carbon atoms of butyl chains of [BMIM] cations, which facilitates their librated motion and hence contributes to their fast diffusion in IL-vacuum interfacial region. Beneath such exposed layer in IL-vacuum interface, the microscopic ionic structure resembles that in the bulk region of confined IL film, and hence exhibits similar dynamical property. The spatial structural heterogeneity of confined ion pairs in interfacial regions contributes directly to the dynamical heterogeneity. Both spatial and dynamical heterogeneities of confined [BMIM][PF_6] ion pairs are important for understanding their performances for example in lubricants, IL-based electrochemical double-layer capacitors and dye-sensitized solar cells.

Acknowledgment

We gratefully acknowledge the financial support from the Swedish Science Council (VR) and generous computing time allocation from SNIC. This work is subsidized by the National Basic Research Program of China (973 Program, 2012CB821500), and supported by National Science Foundation of China (21025416).

Physical Chemistry Chemical Physics Accepted Manuscript

References

1 S. Zhang, N. Sun, X. He, X. Lu and X. Zhang, *J. Phys. Chem. Ref. Data*, 2006, **35**, 1475.

2 C. Largeot, C. Portet, J. Chmiola, P.-L. Taberna, Y. Gogotsi and P. Simon, *J. Am. Chem. Soc.*, 2008, **130**, 2730–2731.

3 M. V. Fedorov and A. A. Kornyshev, *J. Phys. Chem. B*, 2008, **112**, 11868–11872.

4 V. Lockett, R. Sedev, J. Ralston, M. Horne and T. Rodopoulos, *J. Phys. Chem. C*, 2008, **112**, 7486–7495.

5 P. Simon and Y. Gogotsi, *Nature Mater.*, 2008, **7**, 845–854.

6 M. Armand, F. Endres, D. R. MacFarlane, H. Ohno and B. Scrosati, *Nature Mater.*, 2009, **8**, 621–629.

7 J. W. Lee, J. Y. Shin, Y. S. Chun, H. B. Jang, C. E. Song and S. Lee, *Acc. Chem. Res.*, 2010, **43**, 985–994.

8 J. P. Hallett and T. Welton, *Chem. Rev.*, 2011, **111**, 3508.

9 W. Lu, A. G. Fadeev, B. H. Qi, E. Smela, B. R. Mattes, J. Ding, G. M. Spinks, J. Mazurkiewicz, D. Z. Zhou, G. G. Wallace, D. R. MacFarlane, S. A. Forsyth and M. Forsyth, *Science*, 2002, **297**, 983–987.

10 A. Hagfeldt, G. Boschloo, L. Sun, L. Kloo and H. Pettersson, *Chem. Rev.*, 2010, **110**, 6595–6663.

11 S. Y. Lee, A. Ogawa, M. Kanno, H. Nakamoto, T. Yasuda and M. Watanabe, *J. Am. Chem. Soc.*, 2010, **132**, 9764–9773.

12 P. Wang, S. M. Zakeeruddin, I. Exnar and M. Grätzel, *Chem. Commun.*, 2002, 2972–2973.

13 D. Kuang, P. Wang, S. Ito, S. M. Zakeeruddin and M. Grätzel, *J. Am. Chem. Soc.*, 2006, **128**, 7732–7733.

14 M. Gorlov and L. Kloo, *Dalton Trans.*, 2008, 2655–2666.

15 Y. Bai, Y. Cao, J. Zhang, M. Wang, R. Li, P. Wang, S. M. Zakeeruddin and M. Grätzel, *Nature Mater.*, 2008, **7**, 626–630.

16 J. Liu, X. Yang, J. Cong, L. Kloo and L. Sun, *Phys. Chem. Chem. Phys.*, 2012, **14**, 11592–11595.

17 E. Frackowiak, *Phys. Chem. Chem. Phys.*, 2007, **9**, 1774–1785.

18 M. F. El-Kady, V. Strong, S. Dubin and R. B. Kaner, *Science*, 2012, **335**, 1326–1330.

19 L. Liu, S. Li, Z. Cao, Y. Peng, G. Li, T. Yan and X.-P. Gao, *J. Phys. Chem. C*, 2007, **111**, 12161–12164.

20 R. Singh, N. N. Rajput, X. He, J. Monk and F. R. Hung, *Phys. Chem. Chem. Phys.*, 2013, **15**, 16090–16103.

21 M. Sha, F. Zhang, G. Wu, H. Fang, C. Wang, S. Chen, Y. Zhang and J. Hu, *J. Chem. Phys.*, 2008, **128**, 134504.

22 S. Wang, S. Li, Z. Cao and T. Yan, *J. Phys. Chem. C*, 2009, **114**, 990–995.

23 J. Vatamanu, O. Borodin and G. D. Smith, *J. Am. Chem. Soc.*, 2010, **132**, 14825–14833.

24 Y.-L. Wang, A. Laaksonen and Z.-Y. Lu, *Phys. Chem. Chem. Phys.*, 2013, **15**, 13559–13569.

25 N. Sieffert and G. Wipff, *J. Phys. Chem. C*, 2008, **112**, 19590–19603.

26 S. Bovio, A. Podesta, P. Milani, P. Ballone and M. G. Del Pópolo, *J. Phys.: Condens. Matter*, 2009, **21**, 424118.

27 M. Mezger, H. Schröder, H. Reichert, S. Schramm, J. S. Okasinski, S. Schöder, V. Honkimäki, M. Deutsch, B. M. Ocko, J. Ralston, M. Rohwerder, M. Stratmann and H. Dosch, *Science*, 2008, **322**, 424–428.

28 M. Mezger, S. Schramm, H. Schröder, H. Reichert, M. Deutsch, E. J. De Souza, J. S. Okasinski, B. M. Ocko, V. Honkimäki and H. Dosch, *J. Chem. Phys.*, 2009, **131**, 094701.

29 C. Pinilla, M. G. Del Pópolo, R. M. Lynden-Bell and J. Kohanoff, *J. Phys. Chem. B*, 2005, **109**, 17922–17927.

30 R. Singh, J. Monk and F. R. Hung, *J. Phys. Chem. C*, 2011, **115**, 16544–16554.

31 P. Wu, J. Huang, V. Meunier, B. G. Sumpter and R. Qiao, *ACS Nano*, 2011, **5**, 9044–9051.

32 N. N. Rajput, J. Monk, R. Singh and F. R. Hung, *J. Phys. Chem. C*, 2012, **116**, 5169–5181.

33 Y. Shim and H. J. Kim, *ACS Nano*, 2009, **3**, 1693–1702.

34 K. Dong, G. Zhou, X. Liu, X. Yao, S. Zhang and A. Lyubartsev, *J. Phys. Chem. C*, 2009, **113**, 10013–10020.

35 R. Singh, J. Monk and F. R. Hung, *J. Phys. Chem. C*, 2010, **114**, 15478–15485.

36 Y. Shim and H. J. Kim, *ACS Nano*, 2010, **4**, 2345–2355.

37 J. Monk, R. Singh and F. R. Hung, *J. Phys. Chem. C*, 2011, **115**, 3034–3042.

38 N. N. Rajput, J. Monk and F. R. Hung, *J. Phys. Chem. C*, 2012, **116**, 14504–14513.

39 M. H. Kowsari, S. Alavi, M. Ashrafizaadeh and B. Najafi, *J. Chem. Phys.*, 2008, **129**, 224508.

40 H. Liu and E. Maginn, *J. Chem. Phys.*, 2011, **135**, 124507.

41 P. Scheidler, W. Kob and K. Binder, *J. Phys. Chem. B*, 2004, **108**, 6673–6686.

42 W. Smith, C. W. Yong and P. M. Rodger, *Mol. Simul.*, 2002, **28**, 385–471.

43 C. Rey-Castro, A. L. Tormo and L. F. Vega, *Fluid Phase Equilib.*, 2007, **256**, 62–69.

44 H. Zhou, M. Rouha, G. Feng, S. S. Lee, H. Docherty, P. Fenter, P. T. Cummings, P. F. Fulvio, S. Dai, J. McDonough, V. Presser and Y. Gogotsi, *ACS Nano*, 2012, **6**, 9818–9827.

45 K. E. Gubbins, Y.-C. Liu, J. D. Moore and J. C. Palmer, *Phys. Chem. Chem. Phys.*, 2011, **13**, 58–85.

46 Y.-L. Wang, A. Lyubartsev, Z.-Y. Lu and A. Laaksonen, *Phys. Chem. Chem. Phys.*, 2013, **15**, 7701–7712.

47 C. Romero and S. Baldelli, *J. Phys. Chem. B*, 2006, **110**,

This journal is © The Royal Society of Chemistry [year]

Physical Chemistry Chemical Physics Accepted Manuscript

6213–6223.
48 M. R. Castillo, J. M. Fraile and J. A. Mayoral, *Langmuir*, 2012, **28**, 11364–11375.
49 M. Sha, G. Wu, H. Fang, G. Zhu and Y. Liu, *J. Phys. Chem. C*, 2008, **112**, 18584–18587.
50 M. Sha, G. Wu, Q. Dou, Z. Tang and H. Fang, *Langmuir*, 2010, **26**, 12667–12672.
51 Q. Dou, M. Sha, H. Fu and G. Wu, *J. Phys.: Condens. Matter*, 2011, **23**, 175001.
52 J. Sweeney, F. Hausen, R. Hayes, G. B. Webber, F. Endres, M. W. Rutland, R. Bennewitz and R. Atkin, *Phys. Rev. Lett.*, 2012, **109**, 155502.
53 B. L. Bhargava and S. Balasubramanian, *J. Chem. Phys.*, 2007, **127**, 114510.

Physical Chemistry Chemical Physics Accepted Manuscript